Studies On Synthesis And Characterization Of $Cd_{3x}In_{2-2x}S_3$ Alloy Thin Films By Nebulized Spray Pyrolysis Technique

J. Raj Mohamed[1], P. S. Satheeshkumar[2], L. Amalraj[3]

[1]PG & Research Department of Physics, H.H. The Rajah's College, Pudukkottai 622001, Tamilnadu, India

[2,3]PG & Research Department of Physics, V.H.N.S.N. College, Virudhunagar 626001, Tamilnadu, India

[1]raj.shafraz@gmail.com, [2]pssatheesh@yahoo.com, [3]amalraj.raj1973@gmail.com

Abstract **-** Nanostructured $Cd_{3x}In_{2-2x}S_3$ thin films with different concentration of ($0 \leq x \leq 1$) deposited at 300 °C using the NSP technique. The films were characterized by structural, surface, optical and electrical properties, respectively. X-ray diffraction analysis shows that the $Cd_{3x}In_{2-2x}S_3$ films have cubic structure with preferential orientation along (111) plane. The estimated values compare well with the standard values. Micro structural properties of $Cd_{3x}In_{2-2x}S_3$ thin films such as crystallite size, dislocation density, micro strain, number of crystallites and texture coefficient were calculated. The optical band gap value was calculated from transmittance and absorption data. The electrical properties of $Cd_{3x}In_{2-2x}S_3$ thin films are studied and the results are discussed in detail.

Keywords **- $Cd_{3x}In_{2-2x}S_3$ thin films, Nebulized spray pyrolysis, Xrd, SEM, Hall effect, Urbach energy, Skin depth**

I. INTRODUCTION

Group II –VI semiconductor thin films belonging to the cadmium chalcogenide family are reckoned to be very significant materials for a broad spectrum of optoelectronic applications **[1-3]** and photovoltaic applications **[4]** as having precise physical properties such as high coefficient of absorption, direct band gap and good electrical properties. CdS and In_2S_3 are better known wide and direct band gap II-VI and III-VI semiconductors with a band gap, E_g of 2.37-2.44 eV and 2.2-2.68 eV respectively **[5,6]**. The CdS window layer absorbs the blue band of the solar spectrum due to its low band gap which efforts a fall in the solar cell efficiency **[7,8]**. The alloy of Cd-In-S should be more applications because its band gap can be tuned by changing the composition of the elements. In general, thin films have been notably photogenic owing to their potential applications in optoelectronic devices, photovoltaic and solar cell converters. The n-type $CdIn_2S_4$ thin films have recently concentrated considerable attention owing to their exciting physical properties. It has wide applications in optoelectronic devices, photoconductors, solar cells and light emitting diodes (LED) **[9-12]**.

$CdIn_2S_4$ thin films have been grown by various techniques such as vacuum evaporation **[13]**, successive ionic layer absorption and reaction (SILAR) **[14]**, pulse electro deposition **[15]**, electro deposition **[16]**, hot wall epitaxy method **[17,18]**, hydrothermal **[19]**, and spray pyrolysis **[20, 21]** technique. The physical deposition techniques are comparably very expensive and high energy consuming even though it provided quality and uniform films. Nebulized spray pyrolysis technique (NSP) is a simple, cost effective by which an efficient way of growing thin films is possible. In spite of the fact that, a variety of research is being considered for $CdIn_2S_4$ thin films, studies on $Cd_{3x}In_{2-2x}S_3$ ($0 \leq x \leq 1$) thin films are not previously studied. In this work, we report the structural, morphological, optical, elemental and electrical conductivity properties of nebulized spray deposited $Cd_{3x}In_{2-2x}S_3$ ($0 \leq x \leq 1$) thin films.

II. EXPERIMENTAL TECHNIQUE

To study the impact of composition of $Cd_{3x}In_{2-2x}S_3$ thin films on the physical properties while adapting this technique, the following process was preceded.

A. *Materials and methods*

$Cd_{3x}In_{2-2x}S_3$ ($0 \leq x \leq 1$) thin films were deposited on amorphous micro glass substrates by spraying an aqueous solution containing $CdCl_2$, $InCl_3$ (Sigma-Aldridge) and thiourea CS $(NH_2)_2$ (GR E Merck) with nebulized spray pyrolysis technique. In this study, the compositional parameter (x) was adjusted by maintaining the volume concentration of Cd^{2+}, In^{2+}, and S^{2-} ions. The temperature of the substrate was restrained by an iron-constantan thermocouple and maintained constant at its optimized value of 300 °C. The oxygen carrier gas flow rate was kept at 1 kg/cm^2 related to an average pressure solution rate of 5ml per 15 minutes. The precursor solution was kept inside the nebulizer unit. The nebulizer unit was attached to an air compressor. The compressed air is carried out by tubing and stimulates the precursor solution into an "L" glass tube. The mist like tiny droplets of particles was released from the glass tube to deposit onto the glass substrate, which is placed in the uniform hot zone of the furnace. Films are very shiny and yellowish. After deposition, the films were permitted to cool to room temperature and then preserved them in desiccators.

B. *Characterization technique*

The chemical and structural phase of the $Cd_{3x}In_{2-2x}S_3$ ($0 \leq x \leq 1$) films were determined by X-Pert-Pro X-ray diffractometer (Cu Kα, λ=1.5418 Å) over a 2θ range of 10 - 65 °C. The optical absorption spectra were recorded from 300 to 1100 nm wavelength using Hitachi U3410 model UV-Vis-NIR double beam spectrophotometer at room temperature. The absorption coefficient, type of transition, transmittance, direct energy gap, Urbach energy and skin depth were determined from these studies. Scanning electron microscope (SEM) was used to observe the dispersion of particles, rough morphology and the particle size on the surface of the film. The surface morphology of the as-deposited $Cd_{3x}In_{2-2x}S_3$ ($0 \leq x \leq 1$) thin films was examined by SEM (GENISIS MODEL). The chemical composition of Cd, In and S was found by energy dispersive analysis by x-rays (EDAX) on K and L lines. Hall Effect set up was used for measurement of carrier concentration (n), resistivity (ϱ) and Hall mobility (μ) at room temperature. In agreement with Vander Pauw technique, specially designed Hall probe on printed circuit board (PCB) was used to fix the sample of the size 1 x 1 cm^2. Silver paste was employed to assure good electrical contacts. The thickness of the film was determined using stylus profile meter (Mitutoyo, SJ-301).

III. RESULTS AND DISCUSSION

A. *Structural properties*

Generally, CdS and In_2S_3 exist in two crystal structures, namely Wurtzite (Cubic) and Zinc blende (Hexagonal). It has been reported that chemically deposited CdS and In_2S_3 films depending on preparative conditions, show cubic, hexagonal or mixed crystal structures. X-ray diffraction pattern of $Cd_{3x}In_{2-2x}S_3$ thin films at different compositional parameter from x=0.0 to 1.0 is depicted as shown in Fig.1. It is seen that all film samples are polycrystalline over the entire range of composition parameter. For x=0.0 (In_2S_3), the diffraction peaks are along (111), (311), (222), (400), (511) and (444) planes with the standard JCPDS data card **[22]** of the In_2S_3 cubic crystal structure. This type of formation of crystallites was observed by M. Kraini et al. **[23]** for In_2S_3 thin films with the preferred orientation along (111) plane deposited by thermal oxidation of spray pyrolysis technique.

The dominant peaks (111), (222), (511) and (444) shift towards the lower 2θ side, thereby increasing their d values: from 6.2173 to 6.2268Å for (111) plane, from 3.248 to 3.2551Å for (311) plane, from 3.1086 to 3.114Å for (222) plane, from 2.0726 to 2.077 Å for (511) plane and 1.554 to 1.556 Å for (444) plane only with increase in composition parameter (x) to 0.2. From x-ray diffraction pattern, it is observed that $Cd_{3x}In_{2-2x}S_3$ thin films are composed of mixed crystallites of both In_2S_3 and $CdIn_2S_4$. However, the preferred orientation plane (111) is changed from In_2S_3 to $CdIn_2S_4$ cubic crystal structure and remaining peaks belonged to In_2S_3 compound. Compositional parameter at x=0.4, (111), (222), (311), (400), (511) and (440) crystallographic planes with improved crystallinity can be indexed with the mixer of $CdIn_2S_4$ and In_2S_3 crystal structure which was confirmed by the standard data **[24]** and **[22]**. The higher intensity peaks shift further towards the lower 2θ side thereby increasing their d values with increase in the compositional parameter at x=0.6. A comparison of observed and the standard d values for (hkl) planes in JCPDS data **[24]** ensures that cubic structured $CdIn_2S_4$ crystallites were predominant with (111) as preferred orientation plane. R.Horibha **[25]** had obtained similar type of $CdIn_2S_4$ crystallites with (111) preferred orientation plane prepared by vacuum deposition method. The shifting of peak position with the increase in the compositional parameter x=0.8 indicates the formation of alloy system in between CdS and $CdIn_2S_4$ compounds. For x=1.0 (Cd_3S_3), the crystallographic peaks are along (100), (002) and (101) planes with (002) preferential orientation of CdS crystallites as matched with the standard JCPDS data card **[26]**. The average crystalline size and strain for the as-deposited $Cd_{3x}In_{2-2x}S_3$ thin films for the different compositional parameter (x) can be studied by Williamson-Hall plot as shown in Fig.2.

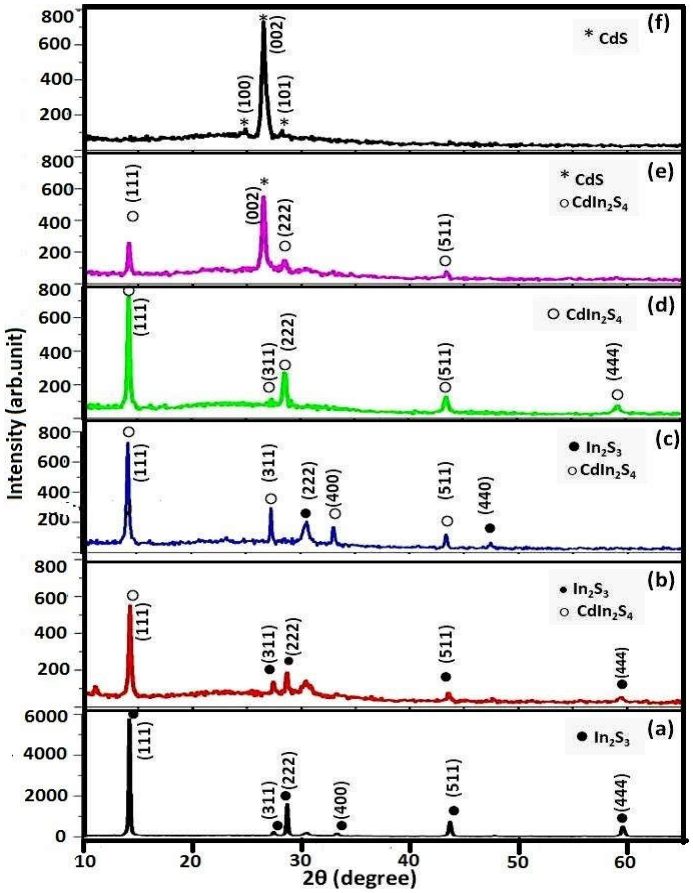

Fig.1 X-ray diffraction pattern of nebulized spray deposited $Cd_{3x}In_{2-2x}S_3$ thin films, with $0.0 \leq x \leq 1.0$

Williamson-Hall analysis is mainly used to split up this size and strain by combining the two equations **[27]**. Eq. (1) stands for the uniform deformation model (UDM),

$$\beta_{hkl} cos\theta = \frac{k\lambda}{D} + 4\varepsilon \, sin\theta \qquad (1)$$

where the strain was assumed uniform in all crystallographic directions. The term (β cosθ) was plotted with respect to (4sinθ) for the peaks of $Cd_{3x}In_{2-2x}S_3$ thin films. Therefore, the slope and y-intercept of the fitted time represent strain and crystallite size respectively. The results of the UDM analysis for the $Cd_{3x}In_{2-2x}S_3$ thin films are shown in Fig.2. The texture coefficient $T_{c(hkl)}$ of the films **[28]** have been calculated from the XRD data using Eq.

$$T_{c\,(hkl)} = \frac{I_0(hkl)}{I_s(hkl)} \left[\frac{1}{N}\sum_{i=1}^{n} \frac{I_0(hkl)}{I_s\,(hkl)}\right]^{-1} \quad (2)$$

The preferred orientation of the films can be confirmed by the higher value of texture coefficient. The increased number of grains along the plane associates the increase in preferred orientations **[29]**. The dislocation density (δ) defined as length of dislocation lines per unit volume of the crystal using crystallite size values (D) has been determined using the Williamson and Smallman's formula **[30]** by Eq.

$$\delta = 1/D^2 \quad lines/m^2 \quad (3)$$

Similarly, the number of crystallites per unit area (N) of the films was determined using the relation **[31]** as given in Eq.

$$N = \frac{t}{D^3} \quad (4)$$

Table1 shows the crystallite size (D), lattice strain (ε), dislocation density (δ), the number of crystallites (N), texture coefficient (T_c) and thickness (t) of $Cd_{3x}In_{2-2x}S_3$ thin films at different compositional parameters from x = 0.0 to 1.0. The average crystallite size (D) of the $Cd_{3x}In_{2-2x}S_3$ thin films can be tuned between 45.47 to 25.13 nm by adjusting the compositional parameter (x) as tabulated in Table1. The micro strain is increased due to the prevailing re-crystallization process in the polycrystalline thin films. Indeed, the observed increase of full width at half maximum (FWHM) of the (111) diffraction peak with an increase of compositional parameter can be ascribed to the decrease particle size. At compositional parameter x = 0.0, a large crystallite size is observed owing to the high mobility of the surface of atoms and increasing cluster formation. The decrease in the crystallite size by increasing 'x' due to the interstitial position of Cd / In atoms. It is observed that the crystallite size decreases and attains a minimum 25.13 nm at x=1.0.

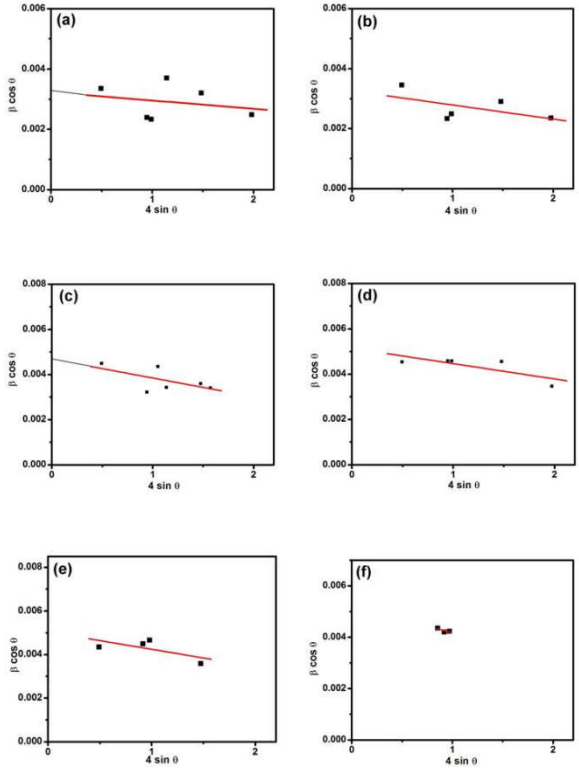

Fig. 2 The Williamson-Hall analysis of $Cd_{3x}In_{2-2x}S_3$ thin films at different compositions ($0 \le x \le 1$) assuming UDM

TABLE1

Structural analysis of $Cd_{3x}In_{2-2x}S_3$ ($0 \leq x \leq 1$) thin films deposited at different compositional parameters (x)

x	*Texture coefficient*	*Crystallite size (nm)*	*Strain X10^{-3}*	*Dislocation density X10^{15} (Lines/m^2)*	*No. of crystallites (m^2)*	*Thickness (nm)*
0.0	5.567	45.47	1.95	0.48	2.6 x10^{15}	245
0.2	3.541	43.60	5.33	0.52	2.8 x10^{15}	236
0.4	3.210	30.76	6.37	1.05	7.6 x10^{15}	224
0.6	2.860	28.52	6.97	1.22	9.8 x10^{15}	216
0.8	2.126	28.02	7.89	1.27	9.9 x10^{15}	207
1.0	2.745	25.13	14.3	1.58	1.2x10^{16}	201

The dislocation density of as-prepared $Cd_{3x}In_{2-2x}S_3$ film increased as 'x' increased. The maximum value of dislocation density is obtained for the film grown compositional parameter x=1.0 (CdS). The change in crystallite size with compositional parameter explained this behavior. Surely, the larger crystallites have a smaller surface to volume ratio thus giving up a lift to the dislocation density. The number of crystallites per unit area (N) depends on the parameters like equidimensional crystallites and the degree of agglomeration of the films. It is observed that the number of crystallites increases as the compositional parameter (x) increases.

B. surface topology

The surface morphology of nebulized spray deposited $Cd_{3x}In_{2-2x}S_3$ ($0 \leq x \leq 1$) thin films was investigated using SEM technique. SEM has been established to be a unique, favorable and versatile method to study surface morphology of thin film. Fig.3 exhibits the SEM micrographs of $Cd_{3x}In_{2-2x}S_3$ ($0 \leq x \leq 1$) thin films prepared at compositional parameter (x) from 0.0 to 1.0. The SEM images were recorded with the same magnification of 30,000 for comparison. It is observed that all the films are uniform without cracks with dense surface morphology covering the whole substrate surface area. The surface morphology of In_2S_3 (Cd=0) thin film is shown in Fig. 3(a). The surface layer of this In_2S_3 thin film is encrusted with more or less large, angular crystals that are unevenly distributed. Fig.3(b) and 3(c) show the surface morphology of $Cd_{3x}In_{2-2x}S_3$(x=0.2 & 0.4) thin films. The entire surface is covered with small with nano-sized angular grains. The surface was distributed with relatively well-chained fibrous structure in the film is grown at x=0.6 shown in Fig. 3(d). The change in morphology is due to the influence of a change in compositional parameter (x). Increasing in compositional parameter (x) to 0.8 improves the surface roughness of the films which is shown in Fig. 3(e). As seen in Fig. 3(f), the surface morphology of Cd_3S_3 thin film which explicit the uneven morphology than other films. The mixture of nano-sized flakes and small spherical like structure are observed throughout the entire surface of the film. All the films comprise most likely aggregates owing to an influence of the change in compositional parameter (x).

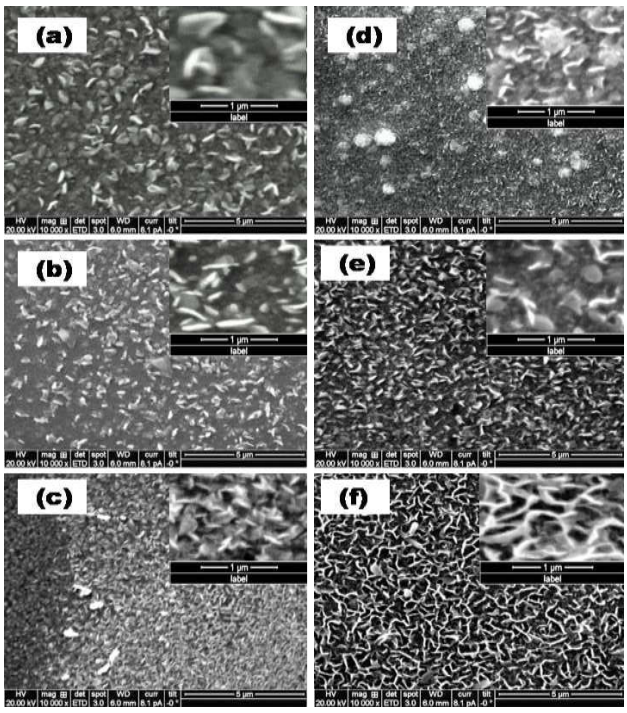

Fig. 3 Scanning electron microscope (SEM) images of $Cd_{3x}In_{2-2x}S_3$ thin films for compositions a) $Cd_{0.0}In_{2.0}S_{3.0}$, b) $Cd_{0.6}In_{1.6}S_{3.0}$, c) $Cd_{1.2}In_{1.2}S_{3.0}$, d) $Cd_{1.8}In_{0.8}S_{3.0}$, e) $Cd_{2.4}In_{0.4}S_3$ and f) $Cd_{3.0}In0.0S_{3.0}$

C. Elemental analysis

The purity and specific composition of $Cd_{3x}In_{2-2x}S_3$ ($0 \leq x \leq 1$) thin films were determined by EDX study, which exposed the presence of Cd, In and S as elementary components. The characteristic EDX spectra of $Cd_{3x}In_{2-2x}S_3$ ($0 \leq x \leq 1$) thin films are shown in Fig.4a-e, respectively. The quantitative atomic percentage of the compositional elements such as Cd, In and S present in $Cd_{3x}In_{2-2x}S_3$ ($0 \leq x \leq 1$) thin films are presented in Table 2. The elemental analysis supports their nominal percentage and chemical purity of system. The increase of Cd and the decrease of In atomic percentage distinctly point that Cd was properly substituted in In-S lattice. In_2S_3 thin film (Cd=0; x=0.0) is sulfur-rich, but Cd involved In-S thin films show sulfur deficiency and the deficiency gradually raised with Cd concentration and more distortion is created in the lattice. The EDX spectra depict that the atomic percentage is closely equal to their nominal stoichiometry with the experimental error.

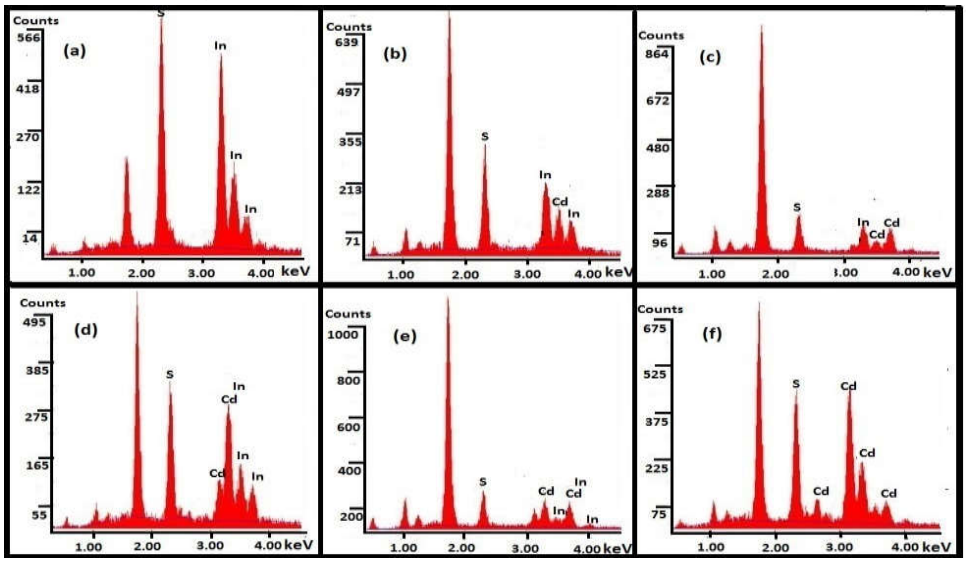

Fig. 4 Energy dispersive X-ray (EDX) pictures of $Cd_{3x}In_{2-2x}S_3$ thin films for compositions a) $Cd_{0.0}In_{2.0}S_{3.0}$, b) $Cd_{0.6}In_{1.6}S_{3.0}$, c) $Cd_{1.2}In_{1.2}S_{3.0}$, d) $Cd_{1.8}In_{0.8}S_{3.0}$, e) $Cd_{2.4}In_{0.4}S_3$ and f) $Cd_{3.0}In0.0S_{3.0}$

TABLE 2

The quantitative analysis of the Weight percentage of the compositional elements presents in the $Cd_{3x}In_{2-2x}S_3$ thin films at different compositional parameters

Composition	***Weight (%)***		
	Cd	***In***	***S***
$Cd_{0.0}In_{2.0}S_3$	-	49.2	50.8
$Cd_{0.6}In_{1.6}S_3$	8.5	33.7	57.7
$Cd_{1.2}In_{1.2}S_3$	21.4	23.1	55.5
$Cd_{1.8}In_{0.8}S_3$	30.2	16.3	53.5
$Cd_{2.4}In_{0.4}S_3$	39.4	8.9	51.7
$Cd_3In_{0.0}S_3$	52.1	-	47.9

D. optical properties

The optical absorption spectra of nebulized spray deposited $Cd_{3x}In_{2-2x}S_3$ ($0 \leq x \leq 1$) thin films have been used to estimate the coefficient of absorption, optical band gap and the nature of transition concerned. The wavelength dependence of the absorption coefficient of $Cd_{3x}In_{2-2x}S_3$ ($0 \leq x \leq 1$) films is shown in Fig. 5. It is found that high optical absorption coefficient ($\alpha = 10^4 cm^{-1}$) was observed for all the compositional parameters. The absorption through the film is comparatively high at below band gap region designating high concentration of defects and free carriers. The absorption reduces suddenly in the long wavelength region. The crisp decrease in absorption is noticed in between 300 – 525 nm which is owing to band edge absorption. The incoming photons have adequate energy to excite electrons for the valence band to conduction band, ensuring in strong absorption in $Cd_{3x}In_{2-2x}S_3$ ($0 \leq x \leq 1$) thin films.

The distinctive room temperature transmittance spectra of $Cd_{3x}In_{2-2x}S_3$ thin films with different compositional parameters from x=0.0 to 1.0 in the wavelength region ranging from 300 to 1100 nm are shown in Fig. 6. The transmittance spectra of $Cd_{3x}In_{2-2x}S_3$ ($0 \leq x \leq 1$) thin films exhibit just opposite tendency of the optical absorption spectra. A close observation displays that all the films show a high transmittance in the visible region (> 450 nm). The variation in transmittance with the compositional parameters (x) is likely ascribed to variation in the film thickness. The transmittance variation is helpful for the window material fabrication in solar cells. The optical band gap of as-deposited $Cd_{3x}In_{2-2x}S_3$ ($0 \leq x \leq 1$) thin films is calculated by employing the Tauc model **[32]** as in Eq.

$$(\alpha h\nu) = A(h\nu - E_g)^p \qquad (5)$$

For semiconductors, n=1/2, 2, 3/2, 3 values related to the allowed direct, allowed indirect, forbidden direct, and forbidden indirect transition only. Since n=1/2 and the absorption coefficient is of the order of 10^4 cm^{-1} sustains the direct band gap nature of $Cd_{3x}In_{2-2x}S_3$ semiconductor for allowed direct transition. The band gap of $Cd_{3x}In_{2-2x}S_3$($0 \leq x \leq 1$) thin films was found for each film by plotting $(\alpha h\nu)^2$ versus hν and then extrapolating the linear portion to the energy basis at α =0. The Tauc plot is used to determine the band gap of $Cd_{3x}In_{2-2x}S_3$ thin films as in Fig.7. The variation of band gap with compositional parameter (x) is shown in Fig.8. The optical band gap of pure In_2S_3 is found to be 2.70 eV and decreases continuously down to 2.41 eV for CdS.

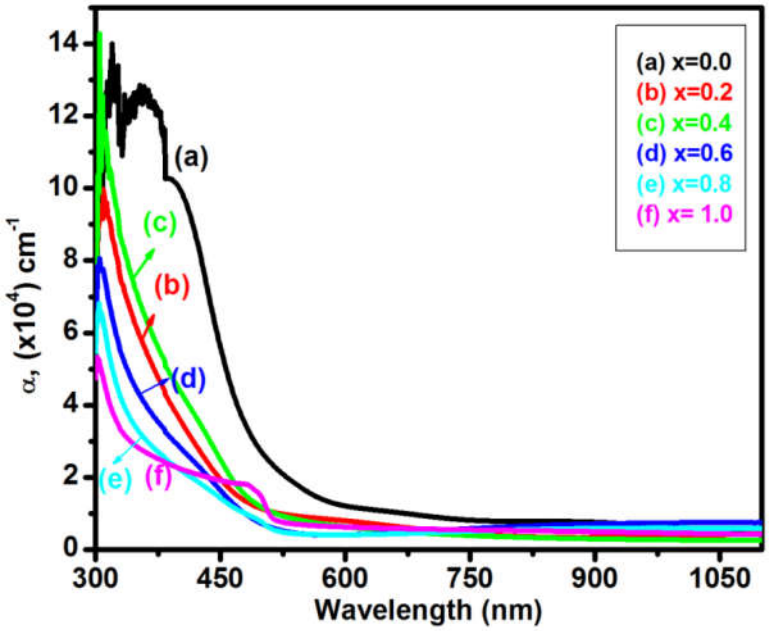

Fig. 5 Absorption coefficient spectra of nebulized spray deposited $Cd_{3x}In_{2-2x}S_3$ thin films, with $0.0 \leq x \leq 1.0$

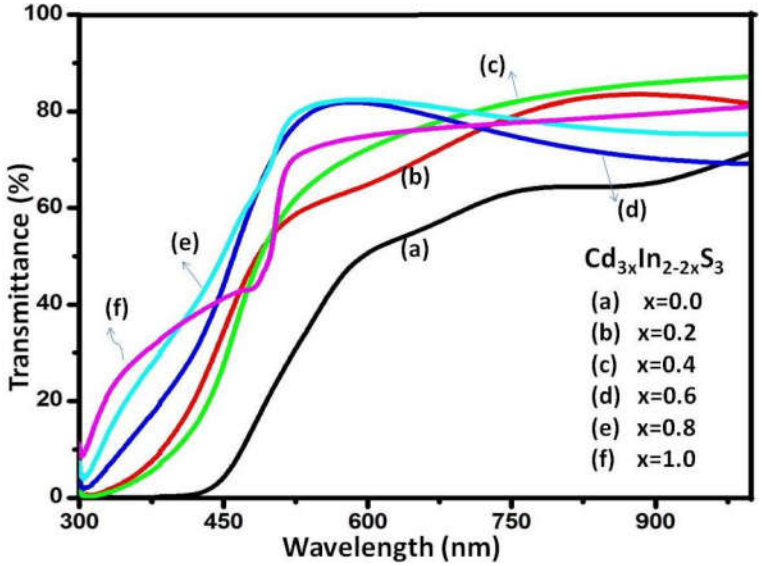

Fig.6 Transmittance spectra of nebulized spray deposited $Cd_{3x}In_{2-2x}S_3$ thin films, with $0.0 \leq x \leq 1.0$

The non-linearity of the variation of band gap with compositions has been previously reported for $Cd_{1-x}Zn_xS$ **[33,34]** and CdSSe **[35]** thin films. The reason for this behavior in this work may be ascribed to slight variation in the film formation, temperature variation and non-stochimetric of the elements. The non-linearity property of as-deposited $Cd_{3x}In_{2-2x}S_3$ thin films can be evaluated using a non-linear equation as in the Eq.

$$y = 0.875\ x^2 - 0.625\ x + 2.75 \qquad (6)$$

This kind of fine variation or tunable band gap properties of $Cd_{3x}In_{2-2x}S_3$ $(0 \leq x \leq 1)$ thin films is suitable for numerous scientific studies and technological applications such as solar cells and optoelectronic devices. The incorporation Cd^{2+} into In-S lattice gives lift to the sulfur deficiency in the lattice as proved by EDX spectra (Fig.4) Cd concentration increases the sulfur deficiency and, therefore, the donor levels get perverted and combine in the conduction band of In_2S_3, making the conduction band to widen the band gap which reduces the band gap.

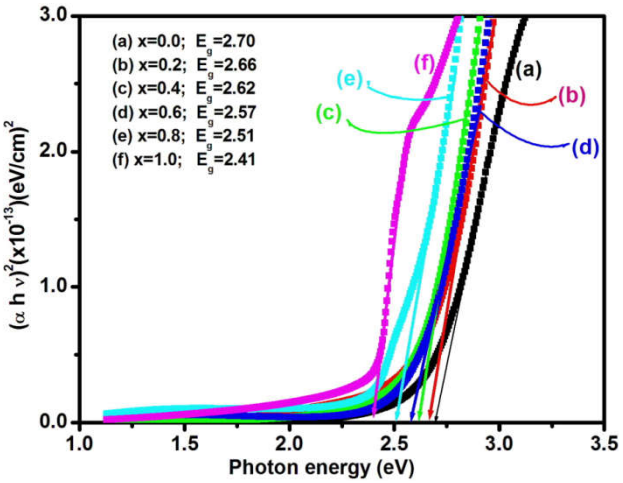

Fig.7 Plot of $(\alpha h\nu)^2$ versus hυ for nebulized spray deposited $Cd_{3x}In_{2-2x}S_3$ thin films, with $0.0 \leq x \leq 1.0$.

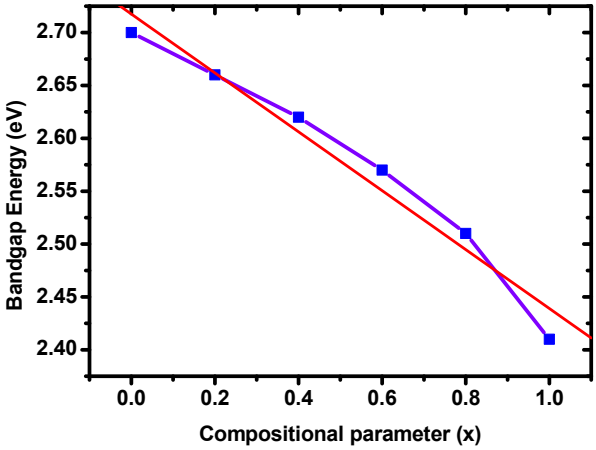

Fig. 8 Variation of band gap energy (eV) with composition with nebulized spray deposited $Cd_{3x}In_{2-2x}S_3$ ($0 \leq x \leq 1$) thin films

The skin depth (s) of the $Cd_{3x}In_{2-2x}S_3$ ($0 \leq x \leq 1$) thin films deposited by nebulized spray pyrolysis technique can be determined by the inverse of the absorption coefficient $s = 2/\alpha = c/\omega k$. The skin depth (s) is really a measure of the distance of penetration of the optical beam of intensity $I=I_0/e^{-x/s}$, into the medium before the beam has deteriorated. Since, s value is of the order of μm, suggesting that the incidental optical beam on material penetrates only very short distance. It is seen from Fig.9 that the skin depth varies from 0.25 to 0.75 μm with compositional parameter (x). The absorption coefficient near the band edge shows an exponential habituation on photon energy and this spectral dependence is determined by the empirical Urbach rule as **[36]** in Eq.

$$\alpha = \alpha_0 \exp(h\nu/E_u) \qquad (7)$$

Fig.10 depicts the plot of ln(α) versus hν by which the Urbach energy E_u have been determined and the values are listed in Table 3. E_u values are continuously increased from 0.62 to 1.98 as the compositional parameter (x) increases that exposed the increased defects in the coating film. In addition, the optical band gap is reversely correlated to the disorder in the film. Hence, an increase in E_u values for the films grown at the compositional parameter (x) from 0.0 to 1.0 can be interpreted with the decrease in E_g values.

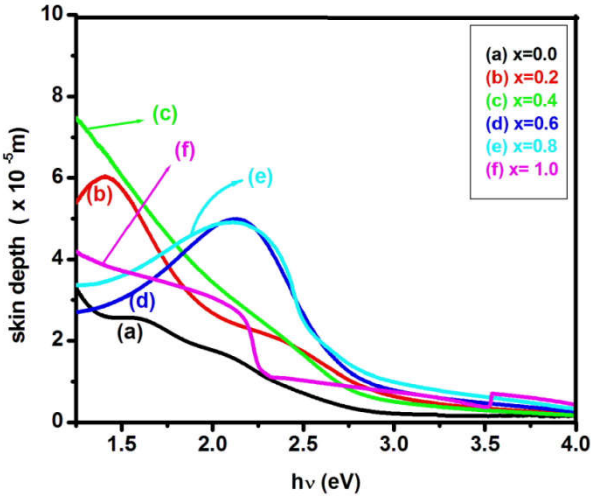

Fig. 9 Variation of skin depth with photon energy of $Cd_{3x}In_{2-2x}S_3$ ($0 \leq x \leq 1$) thin films

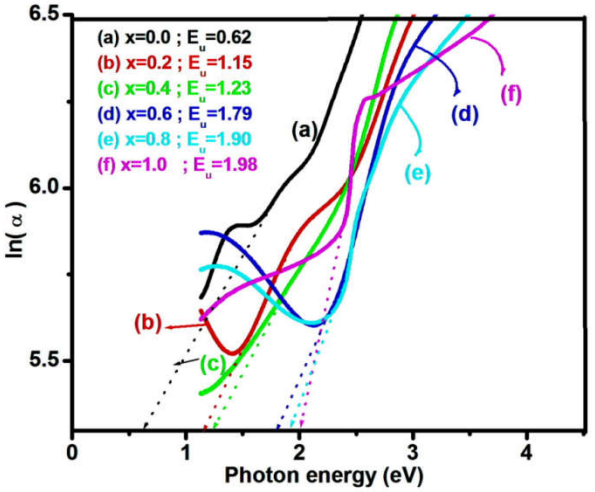

Fig. 10 Plot of ln(α) versus hν for the Urbach energy determination of nebulized spray deposited $Cd_{3x}In_{2-2x}S_3$ thin films, with $0.0 \leq x \leq 1.0$

TABLE 3

Variation of optical and electrical properties of $Cd_{3x}In_{2-2x}S_3$ thin films at different compositional parameters

Composition	***E_g (eV)***	***E_u (eV)***	***Resistivity (Ωcm)***	***Carrier concentration ($x10^{18}(cm^{-3})$)***	***Mobility (cm^2/Vs)***
$Cd_{0.0}In_{2.0}S_3$	2.7	0.62	$7.87x10^{-2}$	7.15	25.4
$Cd_{0.6}In_{1.6}S_3$	2.66	1.15	$9.01x10^{-2}$	6.18	12.8
$Cd_{1.2}In_{1.2}S_3$	2.62	1.23	$1.58x10^{-1}$	5.6	5.32
$Cd_{1.8}In_{0.8}S_3$	2.57	1.79	$1.98x10^{-1}$	3.94	4.40
$Cd_{2.4}In_{0.4}S_3$	2.51	1.90	$2.09x10^{-1}$	3.31	3.88
$Cd_3In_{0.0}S_3$	2.41	1.98	$4.80x10^{-1}$	2.73	1.01

E. Electrical properties

In order to ascertain the carrier concentration, resistivity and Hall mobility including the type of conduction the Hall effect measurement were taken out on the as-deposited $Cd_{3x}In_{2-2x}S_3$ ($0 \leq x \leq 1$) thin films. The Hall Effect measurement is the criterion, dependable and more direct method for finding fundamental electrical properties of semiconductors. Hall Effect measurement brings out that the value of Hall coefficient is negative which adapts that the prepared films have n-type conductivity. Fig. 11 shows the resistivity, Hall mobility and carrier concentration of the films as the function of compositional parameters (x). The electrical resistivity is found to be composition dependent.

The electrical resistivity for In_2S_3 and CdS are $7.87x10^{-2}$ and 4.80×10^{-1} $(\Omega\text{-cm})^{-1}$, respectively. The carrier concentration at room temperature was determined for all the films. The carrier concentration is found to decrease with increase in Cd concentration as shown in Fig.11. The mobility measurements show the $Cd_{3x}In_{2-2x}S_3$ films deposited at x = 0 (In_2S_3) to have higher mobility.

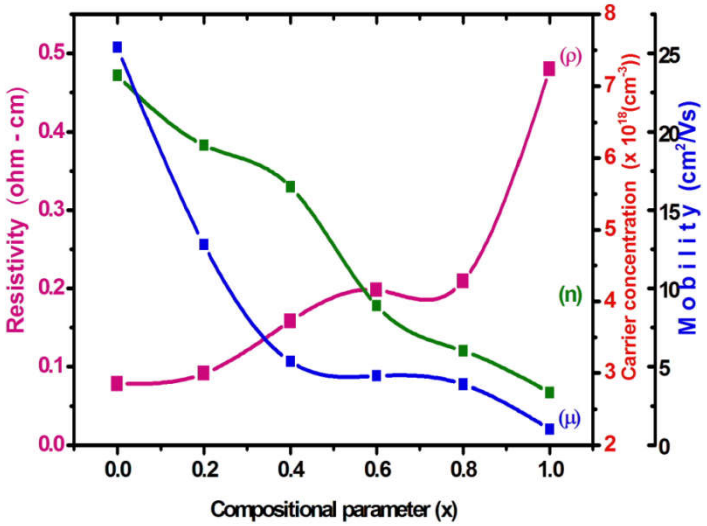

Fig. 11 Variation of resistivity, carrier concentration and mobility of $Cd_{3x}In_{2-2x}S_3$ ($0 \leq x \leq 1$) thin films

This could be understood by reckoning the crystallite size measurements shown in Table 3; the crystallite size of the In_2S_3 thin film (36.84 nm) is much larger than that of the other films which may explicate the higher mobility. Meanwhile, the crystallite size of the other films deposited at compositions (x= 0.4, 0.6 & 0.8) is about the same which may explain why these films have very close mobility values. The mobility values incurred in this work are in agreement with what has been noticed earlier in the literature for polycrystalline In_2S_3 and CdS thin films **[23, 37]**.

IV. CONCLUSION

The variation of composition(x) of various properties of simple and cost effective nebulized spray deposited $Cd_{3x}In_{2-2x}S_3$ ($0 \leq x \leq 1$) thin films was studied in detail. Polycrystalline nature with cubic crystal structure was exposed for all compositions from x-ray diffraction studies. Films with crystallite size in the range of 36.84 - 5.10 nm can be obtained. The smooth variation in crystallite size and energy gap by increasing the compositional parameter (x) made the samples as a promising candidate for the applications of solar cells and optoelectronic devices. Scanning electron microscope studies of $Cd_{3x}In_{2-2x}S_3$ ($0 \leq x \leq 1$) thin films showed polycrystalline texture with intimately smooth surface and evidently defined grains. EDAX study confirmed nearly stoichiometric deposition of $Cd_{3x}In_{2-2x}S_3$ thin films. The absorption spectra of these $Cd_{3x}In_{2-2x}S_3$ composite films showed high transmittance and lower absorption in the visible region illustrated the good optical quality of the crystals which leads to the applications particularly as a window layer in solar cells. The optical parameters such as band gap energy, Skin depth and Urbach energy have been discussed in detail. From the optical studies, the optical band gap was found to decrease with Cd incorporation in In_2S_3 films. The wide and fine tunability of the band gap, as well as uniform changes in the conductivity of the $Cd_{3x}In_{2-2x}S_3$ thin films, have latent applications in many optoelectronic devices. Hall Effect study shows that all films are n-type semiconductors using Hall coefficient values. The carrier concentration of the films is of the order of 10^{18} cm^{-3}. The electrical resistivity of as-deposited $Cd_{3x}In_{2-2x}S_3$ thin films was increased by increasing the composition. The maximum Hall mobility of 25.4 cm^2/Vs was obtained for the film grown at x=1.0 (CdS).

REFERENCES

[1] *G.Sasikala, P.Thilakan, C.Subramaniyan, Sol. Energy Mater. Sol. Cells 62 (2000) 275.*
[2] *P.Roy, S.K.Srivastava, Mater. Chem. Phys., 95 (2006) 235.*
[3] *P.P.Hankare, P.A.Chate, D.J.Sathe, Solid State Sci., 11 (2009) 1226.*
[4] *Hikmat S Hilal, Rania M.A.Ismail, Amer El-Hamouz, Ahed Zyoud, Iyad Saadeddin, Electrochemica Acta, 54 (2009) 3433.*
[5] *J.N.Ximello-Quiebras, G.Contreras-Puente, G.Rueda-Morales, O.Vigil, G.Santana-Rodriguez, A.Morales-Acevedo, Sol. Energy Mater. Sol. Cells, 90 (2006) 727.*
[6] *M.Calixto-Rodriguez, A.Tiburcio-Silver, A.Ortiz, A.Sanchez-Juarez, Thin Solid Films 480-481 (2005) 133.*
[7] *M.C.Baykul, N.Orhan, Thin Solid Films, 518 (2010) 1925.*
[8] *P.Kumar, A.Misra, D.Kumar, D.Dhama, T.P.Sharma, P.N.Dixit, Opt.Mater., 27 (2004) 261.*
[9] *H.Nakanish, Jpn. J.Appl. Phys.19 (1980) 103.*
[10] *S.I. Radautan, V.F.Ithitar, M.I.Shmiglyuk, Savior of Phys. Semicond. 5 (1972) 1959.*
[11] *J.Mu, Q.L.Wei, P.P.Yao, X.L.Zhao, S.Z.Kang, X.C.Li, J. Alloys.Compd. 513 (2012) 506.*
[12] *W.J.Wang, T.W.Ng, W.K.Ho, J.H.Huang, S.J.Liang, T.C.An, G.Y.Li, J.C.Yu, P.K.Wong, Appl. Catal.,B: Environ. 129 (2013) 482.*
[13] *Y.Li, R.Dillert, R.Bahnmann, Thin Solid Films, 516 (2008) 4988.*
[14] *M.Kundakci, A.Ates, A.Astam, M.Yildirim, Physica B, 40 (2008) 600.*
[15] *A.V.Kokate, M.R.Asabe, S.B.Shelake, P.P.Hankare, B.K.Chougule, Physica B, 390 (2007) 84.*
[16] *S.N.Baek, T.S.Jeong, C.J.Youn, K.J.Hong, J.S.Park, D.C.Shin, Y.T.Yoo, J.Cryst.Growth, 262 (2004) 259.*
[17] *S.H.You, K.J.Hong, T.S.Jeong, C.J.Youn, J.S.Park, B.J.Lee, J.W.Jeong, J. Crys.Growth, 271 (2004) 391.*
[18] *W.Zhang, H.Yang, W.Fu, M.Li, Li, W.Yu, J.Alloys.Compd. 561 (2013) 10.*
[19] *R.R.Sawant, K.Y.Rajpure, C.H.Bhosale, Physica B, 393 (2007) 249.*
[20] *G.F.Epps, R.S.Becker, J.Electrochem. Soc. 129 (1982) 2628.*
[21] *X. Fu, G. Wu, S. Song, Z. Song, X. Duo, C. Lin, Appl. Surf. Sci. 148 (1999) 223.*
[22] *R.Mariappan, V.Ponnuswamy, P.Suresh, R.Suresh, M.Ragavendar, Superlattices Microstruct., 59 (2013) 47.*
[23] *M. Kraini, N. Bouguila, I. Halidou, A. Timoumi, S. Alaya, Mat. Sci. Semicond. Process. 16 (2013) 1388.*
[24] *JCPDS diffraction data, file No. 27-0060 & 31-0229.*
[25] *Horiba R, Nakanishi H, Endo S, Jrie T, Surf. Sci. 86 (1979) 498.*
[26] *JCPDS diffraction data, file No. 89-2944.*
[27] *A. Khorsand Zak, W.H. A. Majid, M.E. Abrishami, R. Yousefi, Solid State Sci. 13 (2011) 251.*
[28] *R.Mariappan, V.Ponnuswamy, P.Suresh, R.Suresh, M.Ragavendar, Superlattice. Microst. 59 (2013) 47.*
[29] *R.Suresh, V.Ponnuswamy, R.Mariappan, N.Senthilkumar, Ceram. Int. 40 (2014) 437.*
[30] *G.B.Williamson, R.C.Smallman, Philos.Mag. 1 (1956) 34.*
[31] *R. Anandhi, R. Mohan, K. Swaminathan, K. Ravichandran, Superlattices Microstruct. 51 (2012) 680.*
[32] *J.I.Pankove, Optical Processes in Semiconductors, Prentice and Hall, Inc., New Jersey, pp 36 (1971).*
[33] *S.V.Bose, S.D.Chavan, R.Sharma, J.Alloys. Compd. 436 (2007) 407.*
[34] *L.P.Deshmukh, C.B.Rotti, K.M.Garadkar, P.P.Hankare, B.M.More, D.S.Sutrave, G.S.Shahane, Indian J.Pure Appl.Phys. 35 (1997) 428.*
[35] *K.M.Gadave, C.D.Lokhande, P.P.Hankare, Meter.Chem.Phys. 38 (1994) 393.*
[36] *M.A.Hassan, C.A.Hogarth, J.Mater.Sci., 23 (1988) 2500.*
[37] *Hani Khallaf, Isaiah O.Oladeji, Guangyu Chai, Lee Chow, Thin Solid Films, 516 (2008) 7306.*